

Populate-A-Scene: Affordance-Aware Human Video Generation

Supplementary Material

001 1. Video Results

002 We present the video version of all the data and results we
003 show in the paper, along with additional results, to demon-
004 strate the generalizability of our model. Please refer to
005 the video folder for the results. You can also click on
006 `video_results.html` link to open it with your favorite
007 browser (loading faster in Chrome than Safari!) to see ev-
008 erything all at once. Specifically, we present results of the
009 following kinds:

- 010 • Single-person insertion results.
- 011 • Two-person insertion results.
- 012 • Multi-prompt interaction results.
- 013 • Comparison with image-to-video baselines.

014 We hope those real video results can showcase the qual-
015 ity of our generative model. Note that we tried to not do
016 aggressive cherry picking on those results. All of the shown
017 videos are generated in one pass without tweaking the ran-
018 dom seed, and picked out of around one hundred validation
019 samples to cover a diverse range of interesting behavior.

020 2. Data Processing Details

021 2.1. Data Filtering

022 We get the raw human-related dataset following the prac-
023 tice of video personalization in [5]. Specifically, we first
024 get human videos by selecting videos with human-related
025 concepts in their captions. We extract frames at one-second
026 intervals and apply a face detector to keep videos that con-
027 tain a single face and where the ArcFace cosine similar-
028 ity score [2] between consecutive frames exceeds 0.5. This
029 processing provides us with around one million text-video
030 pairs where a single person appears, with duration from 4s
031 to 16s. We additionally apply OpenPose [1] to only keep
032 those with at least knee joints in the frame to avoid extreme
033 close-ups. At the top of Fig. 1 we show some cases that we
034 discard during the filtering process.

035 Note that interestingly, as we apply all the detection on
036 middle frame, some earlier and later frames might not sat-
037 isfy our requirements of full bodies. We choose to not
038 specifically tackle these edge cases as they tend to have rich
039 interactive contents with large-scale motions.

040 2.2. Human Removal

041 To process the data, we take the first and last frames of a
042 video for human removal to get the scene image.

043 **Human segmentation.** We apply GroundingDINO [4] with
044 the keyword `human` to get bounding boxes for each human

in the image. We apply SAM 2.1 with the bounding box as
045 guidance to segment out the binary human mask.

046 **Inpainting.** We apply the SDXL diffusion inpainting
047 model. To avoid fuzzy segmentation boundary, we use
048 OpenCV to dilate each binary mask by 50 pixels so that
049 it's guaranteed to cover the whole human area. The positive
050 prompt we use is "natural, photorealistic, empty, environ-
051 ment, blank, background, bg", and the negative prompt is
052 "person, human, text". For two people videos, we separate
053 the two person masks, and does inpainting with each mask
054 separately. At the bottom of Fig. 1 we show a few additional
055 data samples, including mask and detected poses.

056 2.3. Prompt Post-processing.

057 We split the prompt by sentences. For each sentence, we
058 ask the LLaMA model [3] whether it describes the person
059 or the background. If it's defined as a background prompt,
060 we remove it from the caption. We additionally remove all
061 sentences with the concept of camera in it, as we are not
062 explicitly modeling any human-camera interaction.

063 3. Implementation Details

064 3.1. Base Model

065 We explain some training details of our base model be-
066 low. Refer to [5] for more illustration. Note that while the
067 training scheme and datasets are the same, we use a much
068 smaller counterpart than the publicly announced Movie Gen
069 model due to resource limitation.

070 We perform generation in a learned latent space rep-
071 resentation of the video. This latent code is of shape
072 $T \times C \times H \times W$. To prepare inputs for the Transformer back-
073 bone, the video latent code is 'patchified' using a 3D convolu-
074 tional layer and then flattened to yield a 1D sequence. The
075 3D convolutional layer uses a kernel size of $k_t \times k_h \times k_w$
076 with a stride equal to the kernel size and projects it into
077 the same dimensions as needed by the Transformer back-
078 bone. Thus, the total number of tokens input to the Trans-
079 former backbone is $THW / (k_t k_h k_w)$. We use $k_t = 1$ and
080 $k_h = k_w = 2$, i.e., we produce 2×2 spatial patches.

081 We use a factorized learnable positional embedding to
082 enable arbitrary size, aspect ratio, and video length. Ab-
083 solute embeddings of D dimensions can be denoted as a
084 mapping $\phi(i) : [0, \text{maxLen}] \rightarrow \mathbb{R}^D$ where i denotes the ab-
085 solute index of the patch. We convert the 'patchified' tokens
086 into separate embeddings ϕ_h, ϕ_w and ϕ_t of spatial h, w , and
087 temporal t coordinates. We define $H_{\text{max}}, W_{\text{max}}$, and T_{max}
088 as the maximum sequence length for each dimension, which
089 corresponds to the maximum spatial size and video length

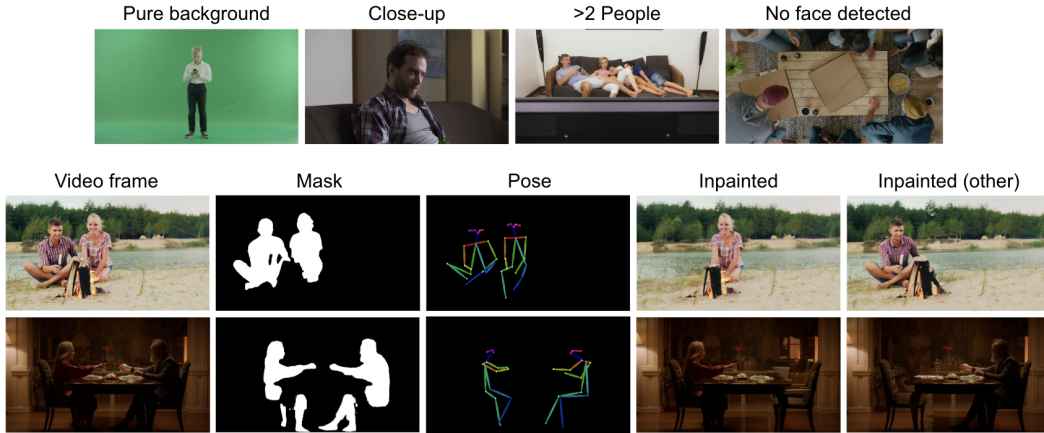


Figure 1. Additional illustration of our data processing pipeline. We include discarded data samples on top, and intermediate outputs of detection and filtering on bottom.

of the patchified inputs. We calculate the final positional embeddings by adding all the factorized positional embeddings together, and finally adding them to the input for all the Transformer layers.

3.2. Conditioning Branch

We build our cross attention conditioning branch by concatenating the text and image features. Specifically, we apply 2 layers of text enhancer self attention, 2 layers of image enhancer deformable attention, then 6 layers of cross-attention with image as key/value and 6 layers of cross-attention with text as key/value. We combine the enhanced image feature with the pre-trained text feature for cross-attention with Transformer layer outputs.

4. Evaluation Details

4.1. Baseline Details

T2I Inpainting. We deploy a pre-trained text-to-image inpainting model on the given scene frame. We use the ground truth human bounding boxes from GroundingDINO’s prediction as a guidance mask for inpainting. Because the baseline’s text encoder is not designed for long prompts, we only take the first two sentences in our caption as the positive inpainting prompt. In practice, they are able to describe the human action and appearance adequately. Note that this is not an exactly fair comparison, as we give the model a ground truth bounding box. We are able to show that, however, our model is able to generate more natural interaction even without a pre-defined position signal.

InstructPix2Pix and AnyV2V. Both of them are based on InstructPix2Pix, except that the second one is an extension into video after editing the first frame. We use LLaMa [3] to rewrite our prompts so that it falls into the instruction distribution. Instead of describing “the video shows a man”,

we rewrite the prompt as “adding a man”. Similarly, due to the limit number of tokens the text encoder can take in, we only rewrite the first two sentences. We use the same prompt for both stages of AnyV2V.

Note that our baselines are mostly trained with squared images. Even though our model is exclusively trained with landscape videos, our Transformer architecture essentially enables generation of arbitrary aspect ratio. To accommodate the baselines, we use squared images for comparison in the main paper. We additionally provide some non-squared comparisons with the two image-based models in the next section.

4.2. Evaluation Metrics

FVD. FVD calculates the feature distance between two sets of videos. (the I3D features). We take the evaluation code and checkpoints from [6]. Specifically, the metric is computed by

$$\text{FVD} = \|\mu_X - \mu_Y\|^2 + \text{Tr} \left(\Sigma_X + \Sigma_Y - 2(\Sigma_X \Sigma_Y)^{1/2} \right)$$

where μ_X , μ_Y are the mean vectors and Σ_X , Σ_Y are the covariance vectors.

CLIP. We compute the CLIP similarity between generated visual contents and the text prompts. For videos, the distance is computed every one second, and averaged across the whole video.

Action Score. We design this metric to eliminate the influence of human appearance and solely evaluate whether the inserted human is doing the correct action. We ask LLaVA-Next [7] what the human is doing in a video, and provide samples of our action prompts as examples. We then compare the CLIP similarity between our prompt and the output. For the static images, we repeat the single static frame to make a video sequence. We notice that, as LLaVA is only

123
124
125
126
127
128
129
130
131
132
133
134
135

136
137
138
139
140
141
142
143
144
145
146
147
148
149

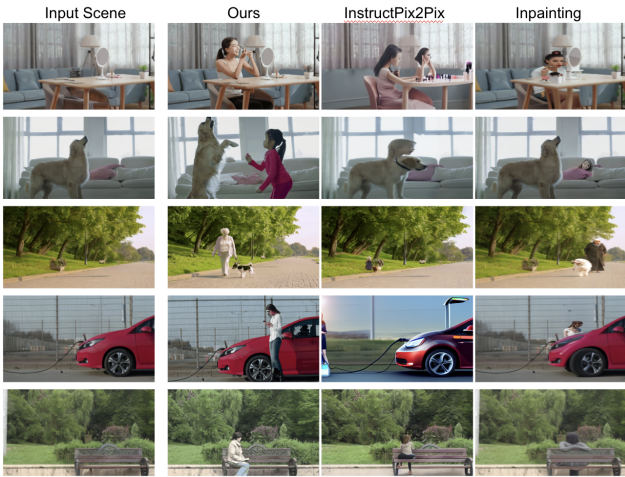


Figure 2. Additional comparison with baselines on non-square image inputs.

150 taking a few key frames to answer the question, repeating
151 the static frames is a reasonable way to decide human ac-
152 tions in an image.

153 4.3. Human Evaluation Details

154 We run a user study to recruit thirty-seven people evaluat-
155 ing the results of our model. We randomly shuffle the re-
156 sults of ours versus the three baselines and the three types
157 of ablations. Among the users, fourteen fill out the small
158 questionnaire with 10 groups of randomly selected results,
159 and twenty-three of them fill out the complete questionnaire
160 with 80 groups. People are asked to select their preference
161 of the results based on four dimensions as described in the
162 main paper.

163 5. Additional Image Baseline Comparison

164 In Fig 2, we show additional frame-wise comparisons with
165 the image-editing baselines to demonstrate our model’s su-
166 perior ability. Note from the results how our model is able
167 to keep the scene consistent instead of generating something
168 semantically similar, and also able to insert a human with-
169 out a mask.

170 6. Ablation Visualizations

171 As shown in Fig. 3, our dual stream conditioning approach
172 with both latent concatenation and feature enhanced cross-
173 attention proves to be the best way of conditioning a T2V
174 model on the scene image. Without latent concatenation,
175 the model generates something semantically similar but not
176 pixel-wise the same. Without fused cross-attention mod-
177 ules, the model is prone to generating distorted, unreason-
178 able motions.

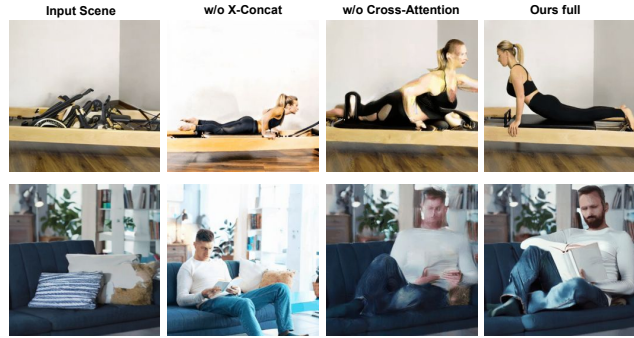


Figure 3. Comparison with alternative designs of our model.

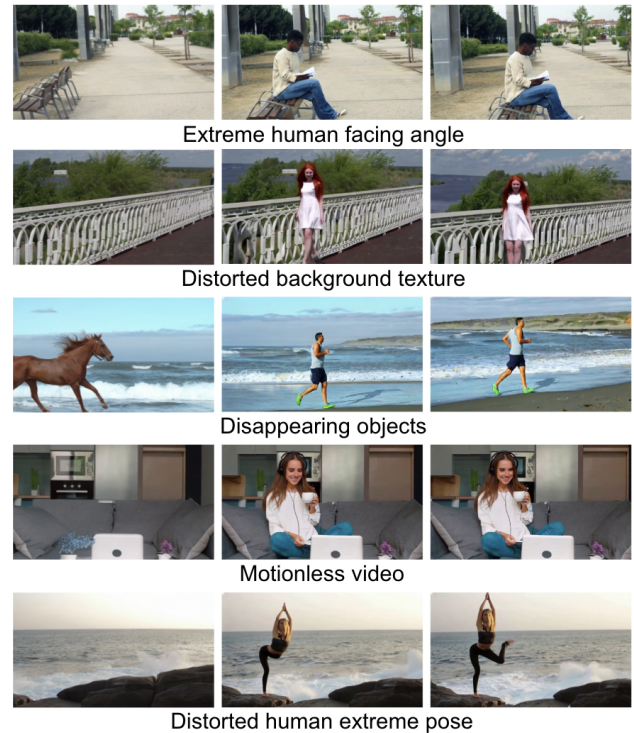


Figure 4. Limitation and failure cases of our model.

179 7. Limitations

180 We discuss a few key limitations and failure cases we no-
181 ticed in our current method. Note that most of them are due
182 to the base text-to-video model’s limited capability, espe-
183 cially as we are basing our work on a smaller, lower reso-
184 lution version. Overall, our method’s quality greatly depends
185 on the base model, and could be further improved with bet-
186 ter model and more computing resources.

187 **Videos with limited motions.** Our model suffers from the
188 common issue of generating videos with limited amount of
189 motions (i.e. static videos). Specifically, we observe that
190 some of our generated results have natural camera move-
191 ments and environmental changes, while having the cen-

192 tral character almost static. This is due to the data dis-
193 tribution which we use to train and fine-tune the model,
194 and can likely be eliminated by providing higher quality
195 fine-tuning dataset, or include motion guidance as an ex-
196 plicit condition to the model. Notably, we notice that our
197 model is able to exhibit fair amount of motion with “action”
198 prompts, like “running”, “walking”, “riking bike” whose
199 underlying semantic requires great movements. And results
200 are more static with “status” prompts like “sitting”, “lying”,
201 which merely describes an existing state. Regardless of the
202 amount of motion, our model is always able to insert the
203 person into the correct place with reasonable interaction.

204 **Human body distortion.** Similar to other text-to-video
205 models, our model is not perfect in generating human move-
206 ments, especially in examples with extreme human motion
207 like doing sports. Specifically, we observe artifacts in limbs
208 and hands when the model expects to generate fine-grained,
209 large-scaled movements. We consider this a common issue
210 of current text-to-video model, and could be improved by
211 using better base model.

212 **Background texture distortion.** We notice that our model
213 fails to keep scene consistent if there is complex geometry
214 or texture in the input image. For example, architectures
215 with repetitive structures, or periodic textures with fine de-
216 tails. This is also an on-going issue of state-of-the-art text-
217 to-video models awaiting solution.

218 **Inpainting artifacts and object disappearing.** Our hu-
219 man removal inpainting algorithms fail on a few edge cases,
220 where it removes the human but replaces it with an ad-
221 ditional object. Training on these data teaches the model
222 to sometimes “remove” existing objects in a scene and re-
223 placing it by a person, even if it shouldn’t disappear in first
224 place. We believe this is a relatively minor data quality issue
225 and could be mitigated by using better inpainting off-the-
226 shelf method, or add an additional round of data filtering.

227 **Extreme human facing angles.** We model is not able to
228 generate back-facing human. This is due to how we fil-
229 ter the data: we detect faces and only keep those with the
230 same face across the whole video, which in nature elimi-
231 nates back facing videos. In cases where the inserted human
232 is expected to face an extreme angle such that most of the
233 faces are unseen from the camera, our model tends to insert
234 person in a wrong direction.

235 8. Reproducibility and Benchmark Release

236 While we are not able to release codebase or dataset due
237 to copyright restrictions, we believe that with detailed de-
238 scriptions of the base models in [5] and the extensive expla-
239 nation of implementation details in this paper could provide
240 the audience with a clear idea of our model’s architecture
241 and training. Moreover, as stated earlier, our goal is not
242 to train the best model, but to explore how pretrained T2V
243 models can perceive affordance from visual signals. We be-

lieve that our conditioning mechanism and cross-attention
244 analysis can be applied to any such open-sourced models
245 as well. We demonstrate results as a proof-of-concept, and
246 hopefully would inspire more explorations in this field. We
247 will release upon acceptance the benchmark dataset that we
248 collected for evaluation to allow fair comparison for follow-
249 up works.
250

251

References

- [1] Z. Cao, G. Hidalgo Martinez, T. Simon, S. Wei, and Y. A. Sheikh. Openpose: Realtime multi-person 2d pose estimation using part affinity fields. *IEEE Transactions on Pattern Analysis and Machine Intelligence*, 2019. 1
- [2] Jiankang Deng, Jia Guo, Niannan Xue, and Stefanos Zafeiriou. Arcface: Additive angular margin loss for deep face recognition. In *Proceedings of the IEEE/CVF Conference on Computer Vision and Pattern Recognition (CVPR)*, 2019. 1
- [3] Abhimanyu Dubey, Abhinav Jauhri, Abhinav Pandey, Abhishek Kadian, Ahmad Al-Dahle, Aiesha Letman, Akhil Mathur, Alan Schelten, Amy Yang, Angela Fan, Anirudh Goyal, Anthony Hartshorn, Aobo Yang, Archi Mitra, Archie Srivankumar, Artem Korenev, Arthur Hinsvark, Arun Rao, Aston Zhang, Aurelien Rodriguez, Austen Gregerson, Ava Spataru, Baptiste Roziere, Bethany Biron, Binh Tang, Bobbie Chern, Charlotte Caucheteux, Chaya Nayak, Chloe Bi, Chris Marra, Chris McConnell, Christian Keller, Christophe Touret, Chunyang Wu, Corinne Wong, Cristian Canton Ferrer, Cyrus Nikolaidis, Damien Allonsius, Daniel Song, Danielle Pintz, Danny Livshits, David Esioubi, Dhruv Choudhary, Dhruv Mahajan, Diego Garcia-Olano, Diego Perino, Dieuwke Hupkes, Egor Lakomkin, Ehab AlBadawy, Elina Lobanova, Emily Dinan, Eric Michael Smith, Filip Radenovic, Frank Zhang, Gabriel Synnaeve, Gabrielle Lee, Georgia Lewis Anderson, Graeme Nail, Gregoire Mialon, Guan Pang, Guillem Cucurell, Hailey Nguyen, Hannah Korevaar, Hu Xu, Hugo Touvron, Iliyan Zarov, Imanol Arrieta Ibarra, Isabel Kloemann, Ishan Misra, Ivan Evtimov, Jade Copet, Jaewon Lee, Jan Gefert, Jana Vranes, Jason Park, Jay Mahadeokar, Jeet Shah, Jelmer van der Linde, Jennifer Billock, Jenny Hong, Jenya Lee, Jeremy Fu, Jianfeng Chi, Jianyu Huang, Jiawen Liu, Jie Wang, Jiecao Yu, Joanna Bitton, Joe Spisak, Jongsoo Park, Joseph Rocca, Joshua Johnstun, Joshua Saxe, Junting Jia, Kalyan Vasudevan Alwala, Kartikeya Upasani, Kate Plawiak, Ke Li, Kenneth Heafield, Kevin Stone, Khalid El-Arini, Krithika Iyer, Kshitiz Malik, Kuenley Chiu, Kunal Bhalla, Lauren Rantala-Yeary, Laurens van der Maaten, Lawrence Chen, Liang Tan, Liz Jenkins, Louis Martin, Lovish Madaan, Lubo Malo, Lukas Blecher, Lukas Landzaat, Luke de Oliveira, Madeline Muzzi, Mahesh Pasupuleti, Mannat Singh, Manohar Paluri, Marcin Kardas, Mathew Oldham, Mathieu Rita, Maya Pavlova, Melanie Kambadur, Mike Lewis, Min Si, Mitesh Kumar Singh, Mona Hassan, Naman Goyal, Narjes Torabi, Nikolay Bashlykov, Nikolay Bogoychev, Niladri Chatterji, Olivier Duchenne, Onur Çelebi, Patrick Alrassy, Pengchuan Zhang, Pengwei Li, Petar Vasic, Peter Weng, Prajjwal Bhargava, Pratik Dubal, Praveen Krishnan, Punit Singh Koura, Puxin Xu, Qing He, Qingxiao Dong, Ragavan Srinivasan, Raj Ganapathy, Ramon Calderer, Ricardo Silveira Cabral, Robert Stojnic, Roberta Raileanu, Rohit Girdhar, Rohit Patel, Romain Sauvestre, Ronnie Polidoroff, Roshan Sumbaly, Ross Taylor, Ruan Silva, Rui Hou, Rui Wang, Saghar Hosseini, Sahana Chennabasappa, Sanjay Singh, Sean Bell, Seohyun Sonja Kim, Sergey Edunov, Shaoliang Nie, Sharan Narang, Sharath Raparthi, Sheng Shen, Shengye Wan, Shruti Bhosale, Shun Zhang, Simon Vandenhende, Soumya Batra, Spencer Whit-

- man, Sten Sootla, Stephane Collot, Suchin Gururangan, Sydney Borodinsky, Tamar Herman, Tara Fowler, Tarek Sheasha, Thomas Georgiou, Thomas Scialom, Tobias Speckbacher, Todor Mihaylov, Tong Xiao, Ujjwal Karn, Vedanuj Goswami, Vibhor Gupta, Vignesh Ramanathan, Viktor Kerkez, Vincent Gonguet, Virginie Do, Vish Vogeti, Vladan Petrovic, Weiwei Chu, Wenhan Xiong, Wenjin Fu, Whitney Meers, Xavier Martinet, Xiaodong Wang, Xiaoqing Ellen Tan, Xinfeng Xie, Xuchao Jia, Xuewei Wang, Yaelle Goldschlag, Yashesh Gaur, Yasmine Babaei, Yi Wen, Yiwen Song, Yuchen Zhang, Yue Li, Yuning Mao, Zacharie Delpierre Coudert, Zheng Yan, Zhengxing Chen, Zoe Papakipos, Aditya Singh, Aaron Grattafiori, Abha Jain, Adam Kelsey, Adam Shajnfeld, Adithya Gangidi, Adolfo Victoria, Ahuva Goldstand, Ajay Menon, Ajay Sharma, Alex Boesenberg, Alex Vaughan, Alexei Baevski, Allie Feinstein, Amanda Kallet, Amit Sangani, Anam Yunus, Andrei Lupu, Andres Alvarado, Andrew Caples, Andrew Gu, Andrew Ho, Andrew Poulton, Andrew Ryan, Ankit Ramchandani, Annie Franco, Aparajita Saraf, Arkabandhu Chowdhury, Ashley Gabriel, Ashwin Bharambe, Assaf Eisenman, Azadeh Yazdan, Beau James, Ben Maurer, Benjamin Leonhardi, Bernie Huang, Beth Loyd, Beto De Paola, Bhargavi Paranjape, Bing Liu, Bo Wu, Boyu Ni, Braden Hancock, Bram Wasti, Brandon Spence, Brani Stojkovic, Brian Gamido, Britt Montalvo, Carl Parker, Carly Burton, Catalina Mejia, Changhan Wang, Changkyu Kim, Chao Zhou, Chester Hu, Ching-Hsiang Chu, Chris Cai, Chris Tindal, Christoph Feichtenhofer, Damon Civin, Dana Beaty, Daniel Kreymer, Daniel Li, Danny Wyatt, David Adkins, David Xu, Davide Testuggine, Delia David, Devi Parikh, Diana Liskovich, Didem Foss, Dingkang Wang, Duc Le, Dustin Holland, Edward Dowling, Eissa Jamil, Elaine Montgomery, Eleonora Presani, Emily Hahn, Emily Wood, Erik Brinkman, Esteban Arcaute, Evan Dunbar, Evan Smothers, Fei Sun, Felix Kreuk, Feng Tian, Firat Ozgenel, Francesco Caggioni, Francisco Guzmán, Frank Kanayet, Frank Seide, Gabriela Medina Florez, Gabriella Schwarz, Gada Badeer, Georgia Swee, Gil Halpern, Govind Thattai, Grant Herman, Grigory Sizov, Guangyi, Zhang, Guna Lakshminarayanan, Hamid Shojanazeri, Han Zou, Hannah Wang, Hanwen Zha, Haroun Habeeb, Harrison Rudolph, Helen Suk, Henry Aspergren, Hunter Goldman, Ibrahim Damlaj, Igor Molybog, Igor Tufanov, Irina-Elena Veliche, Itai Gat, Jake Weissman, James Geboski, James Kohli, Japhet Asher, Jean-Baptiste Gaya, Jeff Marcus, Jeff Tang, Jennifer Chan, Jenny Zhen, Jeremy Reizenstein, Jeremy Teboul, Jessica Zhong, Jian Jin, Jingyi Yang, Joe Cummings, Jon Carvill, Jon Shepard, Jonathan McPhie, Jonathan Torres, Josh Ginsburg, Junjie Wang, Kai Wu, Kam Hou U, Karan Saxena, Karthik Prasad, Kartikay Khandelwal, Katayoun Zand, Kathy Matosich, Kaushik Veeraraghavan, Kelly Michelena, Keqian Li, Kun Huang, Kunal Chawla, Kushal Lakhota, Kyle Huang, Lailin Chen, Lakshya Garg, Lavender A, Leandro Silva, Lee Bell, Lei Zhang, Liangpeng Guo, Licheng Yu, Liron Moshkovich, Luca Wehrstedt, Madijan Khabsa, Manav Avalani, Manish Bhatt, Maria Tsimpoukelli, Martynas Mankus, Matan Hasson, Matthew Lennie, Matthias Reso, Maxim Groshev, Maxim Naumov, Maya Lathi, Meghan Keneally, Michael L. Seltzer, 308
309
310
311
312
313
314
315
316
317
318
319
320
321
322
323
324
325
326
327
328
329
330
331
332
333
334
335
336
337
338
339
340
341
342
343
344
345
346
347
348
349
350
351
352
353
354
355
356
357
358
359
360
361
362
363
364
365

- 366 Michal Valko, Michelle Restrepo, Mihir Patel, Mik Vyatskov,
367 Mikayel Samvelyan, Mike Clark, Mike Macey, Mike Wang,
368 Miquel Jubert Hermoso, Mo Metanat, Mohammad Rastegari,
369 Munish Bansal, Nandhini Santhanam, Natascha Parks,
370 Natasha White, Navyata Bawa, Nayan Singhal, Nick Egebo,
371 Nicolas Usunier, Nikolay Pavlovich Laptev, Ning Dong, Ning
372 Zhang, Norman Cheng, Oleg Chernoguz, Olivia Hart, Omkar
373 Salpekar, Ozlem Kalinli, Parkin Kent, Parth Parekh, Paul
374 Saab, Pavan Balaji, Pedro Rittner, Philip Bontrager, Pierre
375 Roux, Piotr Dollar, Polina Zvyagina, Prashant Ratanchandani,
376 Pritish Yuvraj, Qian Liang, Rachad Alao, Rachel Rodriguez,
377 Rafi Ayub, Raghotham Murthy, Raghu Nayani, Rahul Mitra,
378 Raymond Li, Rebekkah Hogan, Robin Battey, Rocky Wang,
379 Rohan Maheswari, Russ Howes, Ruty Rinott, Sai Jayesh
380 Bondu, Samyak Datta, Sara Chugh, Sara Hunt, Sargun
381 Dhillon, Sasha Sidorov, Satadru Pan, Saurabh Verma, Seiji
382 Yamamoto, Sharadh Ramaswamy, Shaun Lindsay, Shaun
383 Lindsay, Sheng Feng, Shenghao Lin, Shengxin Cindy Zha,
384 Shiva Shankar, Shuqiang Zhang, Shuqiang Zhang, Sinong
385 Wang, Sneha Agarwal, Soji Sajuyigbe, Soumith Chintala,
386 Stephanie Max, Stephen Chen, Steve Kehoe, Steve Saterfield,
387 Sudarshan Govindaprasad, Sumit Gupta, Sungmin
388 Cho, Sunny Virk, Suraj Subramanian, Sy Choudhury, Sydney
389 Goldman, Tal Remez, Tamar Glaser, Tamara Best, Thilo
390 Kohler, Thomas Robinson, Tianhe Li, Tianjun Zhang, Tim
391 Matthews, Timothy Chou, Tzook Shaked, Varun Vontimitta,
392 Victoria Ajayi, Victoria Montanez, Vijai Mohan, Vinay Satish
393 Kumar, Vishal Mangla, Vitor Albiero, Vlad Ionescu, Vlad
394 Poenaru, Vlad Tiberiu Mihailescu, Vladimir Ivanov, Wei Li,
395 Wencheng Wang, Wenwen Jiang, Wes Bouaziz, Will Consta-
396 ble, Xiaocheng Tang, Xiaofang Wang, Xiaojian Wu, Xiaolan
397 Wang, Xide Xia, Xilun Wu, Xinbo Gao, Yanjun Chen, Ye Hu,
398 Ye Jia, Ye Qi, Yenda Li, Yilin Zhang, Ying Zhang, Yossi Adi,
399 Youngjin Nam, Yu, Wang, Yuchen Hao, Yundi Qian, Yuzi He,
400 Zach Rait, Zachary DeVito, Zef Rosnbrick, Zhaoduo Wen,
401 Zhenyu Yang, and Zhiwei Zhao. The llama 3 herd of mod-
402 els, 2024. 1, 2
- [4] Shilong Liu, Zhaoyang Zeng, Tianhe Ren, Feng Li, Hao
404 Zhang, Jie Yang, Chunyan Li, Jianwei Yang, Hang Su, Jun
405 Zhu, et al. Grounding dino: Marrying dino with grounded
406 pre-training for open-set object detection. *arXiv preprint*
407 *arXiv:2303.05499*, 2023. 1
- [5] Adam Polyak, Amit Zohar, Andrew Brown, Andros Tjandra,
409 Animesh Sinha, Ann Lee, Apoorv Vyas, Bowen Shi,
410 Chih-Yao Ma, Ching-Yao Chuang, David Yan, Dhruv Choud-
411 hary, Dingkang Wang, Geet Sethi, Guan Pang, Haoyu Ma,
412 Ishan Misra, Ji Hou, Jialiang Wang, Kiran Jagadeesh, Kun-
413 peng Li, Luxin Zhang, Mannat Singh, Mary Williamson, Matt
414 Le, Matthew Yu, Mitesh Kumar Singh, Peizhao Zhang, Pe-
415 ter Vajda, Quentin Duval, Rohit Girdhar, Roshan Sumbaly,
416 Sai Saketh Rambhatla, Sam Tsai, Samaneh Azadi, Samyak
417 Datta, Sanyuan Chen, Sean Bell, Sharadh Ramaswamy, Shelly
418 Sheynin, Siddharth Bhattacharya, Simran Motwani, Tao Xu,
419 Tianhe Li, Tingbo Hou, Wei-Ning Hsu, Xi Yin, Xiaoliang
420 Dai, Yaniv Taigman, Yaqiao Luo, Yen-Cheng Liu, Yi-Chiao
421 Wu, Yue Zhao, Yuval Kirstain, Zecheng He, Zijian He, Al-
422 bert Pumarola, Ali Thabet, Artsiom Sanakoyeu, Arun Mallya,
423 Baishan Guo, Boris Araya, Breena Kerr, Carleigh Wood, Ce
Liu, Cen Peng, Dmitry Vengertsev, Edgar Schonfeld, El-
424 liot Blanchard, Felix Juefei-Xu, Fraylie Nord, Jeff Liang,
425 John Hoffman, Jonas Kohler, Kaolin Fire, Karthik Sivaku-
426 mar, Lawrence Chen, Licheng Yu, Luya Gao, Markos Geor-
427 gopoulos, Rashel Moritz, Sara K. Sampson, Shikai Li, Simone
428 Parmeggiani, Steve Fine, Tara Fowler, Vladan Petrovic, and
429 Yuming Du. Movie gen: A cast of media foundation models,
430 2024. 1, 4
- [6] Vikram Voleti, Alexia Jolicoeur-Martineau, and Christopher
431 Pal. Mcvd: Masked conditional video diffusion for predic-
432 tion, generation, and interpolation. In *(NeurIPS) Advances in*
433 *Neural Information Processing Systems*, 2022. 2
- [7] Yuanhan Zhang, Bo Li, haotian Liu, Yong jae Lee, Liangke
434 Gui, Di Fu, Jiashi Feng, Ziwei Liu, and Chunyuan Li. Llava-
435 next: A strong zero-shot video understanding model, 2024.
436 2